



ELSEVIER

Carbohydrate Polymers 51 (2003) 37–45

Carbohydrate  
Polymers[www.elsevier.com/locate/carbpol](http://www.elsevier.com/locate/carbpol)

## Aggregation behaviour of polygalacturonic acid in aqueous solution

M. Alonso-Mougán<sup>a</sup>, F. Fraga<sup>b</sup>, F. Meijide<sup>a</sup>, E. Rodríguez-Núñez<sup>b,\*</sup>, J. Vázquez-Tato<sup>a</sup><sup>a</sup>Departamento de Química Física, Facultad de Ciencias, Universidad de Santiago de Compostela, Campus Universitario, 27002 Lugo, Spain<sup>b</sup>Departamento de Física Aplicada, Facultad de Ciencias, Universidad de Santiago de Compostela, Campus Universitario, 27002 Lugo, Spain

Received 20 November 2001; revised 17 April 2002; accepted 18 April 2002

### Abstract

Static and dynamic light scattering techniques have been used to study the aggregation behaviour of polygalacturonic acid (PG) in aqueous solution at different pH values. The dependence of apparent molecular weight, radius of gyration and hydrodynamic radius with time or concentration have been determined. Other structural parameters as contour length, Kuhn segment numbers, mass per unit length, persistence length, and average number of chains per cross section have been deduced from Casassa–Holtzer plots. The weight average molecular weight increases linearly with time suggesting that the aggregation kinetics follows a simple Smoluchowski equation in which all the kernels are identical, the aggregation rate being approximately two chains per day at pH 3.83. As a consequence of this growth the polydispersity of the aggregates increases with time. The growth of the hydrodynamic radius with time suggests that no water molecules remain trapped in the aggregate, explaining why the PG does not gel. © 2003 Elsevier Science Ltd. All rights reserved.

**Keywords:** Polygalacturonic acid; Aggregation behaviour; Light scattering

### 1. Introduction

The interest in the study of aggregation phenomena has grown very much during the last years (Meakin, 1992). Static and dynamic light scattering (SLS and QLS) are excellent techniques for the determination of aggregation rates because they allow the analysis of the evolution of particles without disturbing the aggregation process. Several examples can be found in the literature concerning the use of QLS for measuring aggregation kinetics (Scurthenberger & Newman, 1993), but simultaneous experiments using SLS and QLS are less common (Holthoff, Egelhaaf, Borkovec, Schurtenberger, & Sticher, 1996). This is partly due to the fact that the measurement time of both SLS and QLS in conventional scattering instruments is rather long compared with the kinetic process and, as a consequence, the molecular weight and the mean size of the growing particle are uncertain. The results can only be acceptable if the aggregation process is slow compared with the time required for carrying out the measurement. However, the advantages of using SLS and QLS simultaneously are obvious. For instance, many aggregates have a fractal nature and therefore relationships with molecular

weight ( $M_w$ ), gyration radius ( $R_g$ ) and hydrodynamic radius ( $R_h$ ) can be found (Meakin, 1992).  $R_g$  and  $M_w$  can be measured from SLS experiments but  $R_h$  has to be measured from QLS. Furthermore, the important parameter introduced by Burchard, Schmidt, and Stockmayer (1980),  $\rho = R_g/R_h$ , which provides a simple test for the particle shape, requires the determination of both gyration and hydrodynamic radii, and therefore the use of both scattering techniques.

When working with biopolymers such as polysaccharides it is not easy to find a set of chains with different molecular weights in order to test the relationships between the molecular weight and other structural parameters. Furthermore, as many polysaccharides form gels and aggregates (Burchard, 1994a,b; Lang & Burchard, 1993; Rees, 1969), it is rather difficult to obtain experimental data for isolated chains and test previous relationships (Burchard et al., 1980; Morris, 1991). Pectins (Clark & Ross-Murphy, 1987),  $\beta$ -glucanes (Gómez, Navarro, Manzanares, Horta, & Carbonell, 1997), tamarind seed polysaccharide (Lang & Burchard, 1993), etc. are good examples of that problem. Although structures for aggregates of different polysaccharides have been proposed (Clark & Ross-Murphy, 1987; Walkinshaw & Arnott, 1981a,b), as far as we know nothing is known about the kinetic evolution of the aggregation process.

\* Corresponding author. Tel.: +34-82-223325x24080; fax: +34-82-224904.

E-mail address: faeugen@lugo.usc.es (E. Rodríguez-Núñez).

In this paper we study the aggregation kinetics of polygalacturonic acid (PG) in aqueous solution at different pH values, determining the variation of several structural parameters with time. PG is the skeleton chain of pectins, an important group of polysaccharides in food manufacturing because of their gelling and thickening properties (Clark & Ross-Murphy, 1987). The advantages of the simultaneous use of SLS and QLS techniques are also shown. Finally, a dimensionless parameter,  $\phi$ , defined as the contour length relative to the radius of gyration of the particle, is introduced. The value of this parameter depends only on the structure of the particle, being independent of its molecular weight or its chemical nature. It provides a simple test for the particle shape. Compared with the Burchard parameter,  $\rho$ , it has the advantage of only requiring SLS experiments.

### 1.1. Theoretical background

#### 1.1.1. Static light scattering

In SLS experiments, the intensity of the scattered light is measured at different scattering angles. Traditionally the experimental results have been analyzed through the well known Zimm (1948) equation

$$\frac{Kc}{\Delta R(\theta)} = \frac{1}{M_w} \left( 1 + \frac{q^2 \langle R_g^2 \rangle}{3} + \dots \right) + 2A_2c + \dots \quad (1)$$

In this equation  $\Delta R(\theta)$  is the excess Rayleigh ratio,  $c$  the particle concentration (mass/volume),  $q$  the wave vector,  $M_w$  the weight average molecular weight of the particles in solution,  $R_g$ , the radius of gyration,  $A_2$  the second virial coefficient and  $K$  is given by

$$K = \frac{4\pi^2 \bar{n}_1^2}{N_A \lambda^4} \left( \frac{d\bar{n}}{dc} \right)^2 \quad (2)$$

$d\bar{n}/dc$  is the refractive index increment,  $\lambda$  the wavelength of the incident light and  $\bar{n}_1$  the solvent refractive index.

However, several specific plots have been proposed to obtain detailed information on the structure of the scattering particle (Meakin, 1992). Berry (1966) suggested plotting  $(Kc/R_\theta)^{1/2}$  against  $q^2$ , which for branched materials produces good linearity, at least in the region of small  $q^2$ . As in the Zimm plot, the radius of gyration is obtained from the slope of the plot.

Kuhn (1934) has described a stiff chain by statistical segments of length  $l_K$  greater than the bond length  $l$ . If the number of Kuhn segments  $N_K$  per chain is large enough as to apply the Gaussian statistics, the mean square radius of gyration is given by

$$R_g^2 = \frac{1}{6} N l^2 C_\infty \quad (3)$$

where  $C_\infty = 6R_{g,\theta}^2/l^2 N$  is the characteristic ratio defined by Flory (1969), and the subscript  $\theta$  refers to the theta state and  $N$  is the number of bonds of length  $l$ . The parameters  $N_K$  and

$l_K$  have to fulfill the condition that the contour length should be the same. From previous equations it follows that  $l_K = lC_\infty$  and  $N_K = N/C_\infty$ .

If the chain is short and the Gaussian statistics cannot be applied, for polydisperse chains obeying the Schulz–Flory distribution, the simple relationship

$$\frac{\langle r_g^2 \rangle_z}{l_K^2} = \frac{N_{Kw}^2}{4(1 + N_{Kw})} \quad (4)$$

was obtained by Schmidt (1984). Here  $N_{Kw}$  denotes the weight average of Kuhn segment numbers. This relationship is used below to define the contour length relative to the radius of gyration,  $\phi$ .

According to the Kratky and Porod (1949) plot ( $q^2(R_\theta/Kc)$  vs.  $q$ ), the transition from Gaussian to rod behaviour will occur around a  $q^* = l/2\pi l_K$  value at which  $P(q)_{\text{coil}} = P(q)_{\text{rod}}$  (where  $P(q)$  is the particle form factor). That value can be found by extrapolating the Gaussian plateau to large  $q$  and the rod like straight line towards smaller  $q$ . However, when the number of Kuhn segments is low, the plot usually fails and the Casassa–Holtzer ( $q(R_\theta/Kc)$  vs.  $q$ ) plot is preferred. Here, for rod chains a plateau of height  $\pi/qL$  is reached asymptotically. Furthermore, the plot shows a maximum and the ratio maximum height/asymptotic plateau height is a function of the number  $N_K$  of Kuhn segments (Schmidt et al., 1985). The position of the maximum is a function of the polydispersity since for monodisperse chains  $u(qR_g)_{\text{max}} = 1.4$  and for polydisperse chains with a Schulz–Flory distribution  $u_{\text{max}} = 1.73$ . The plateau height has a value of  $\pi M_L$ , where  $M_L = M/L$  is the mass per unit length or the linear mass density. Random coils do not show the asymptote.

Defining the contour length relative to radius of gyration by means of a parameter  $\phi$  according to

$$\phi = L/R_g \quad (5)$$

we can rewrite Eq. (4) as

$$\phi = 2(1 + N_K)^{1/2} \quad (6)$$

Analogously for a random coil, the parameter  $\phi$  is given by

$$\phi = (6N_K)^{1/2} \quad (7)$$

Both equations evidence a simple relationship between this parameter and the weight average of Kuhn segment numbers. Plots of  $\phi$  vs.  $N_K^{1/2}$  or  $(1 + N_K)^{1/2}$  should be linear for a random coil or a wormlike chain, the slopes being 2.45 and 2, respectively.  $\phi$  has an universal character, independent of the chemical structure of the chain and depends only on its stiffness.

The radius of gyration for a cylinder of length  $L$  and

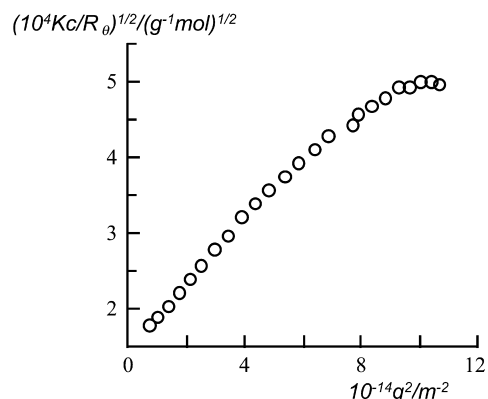


Fig. 1. Berry plot showing a good linearity at low scattering angles. [PG] = 2.5 g dm<sup>-3</sup>. T = 25 °C.

radius  $r$ , is given by

$$R_g = \left( \frac{L^2}{12} + \frac{r^2}{2} \right)^{1/2} \quad (8)$$

while for an ellipsoid of revolution of semi-axis  $a$  and  $b$ ,  $R_g$  is given by

$$R_g = \left( \frac{a^2}{5} + \frac{2b^2}{5} \right)^{1/2} \quad (9)$$

When one of the dimensions of the particle is much higher than the other one ( $L \gg r$  for the cylinder and  $a \gg b$  for a prolate ellipsoid) it is straightforward to show that  $\phi = \sqrt{12} = 3.5$  for a thin rod, and  $\phi = \sqrt{20} = 4.5$  for a thin prolate ellipsoid.

These figures are the maximum values for these geometries, as they decrease when the lower length is not negligible. The minimum values for random coil and wormlike particles correspond to  $N_K = 1$ , i.e.  $\phi = \sqrt{6}$  and  $2\sqrt{2}$ , respectively. Obviously, the comparison between experimental and theoretical values of this parameter will help to distinguish among different shapes of a particle. Therefore as the  $\rho$  parameter,  $\phi$  provides a relatively simple test for the particle shape, although in this case only SLS experiments are required.

### 1.1.2. Dynamic light scattering

In a dynamic or quasi-elastic light scattering experiment, the temporal fluctuations of the scattered intensity, which are due to the Brownian motion of the particles, are analysed (Berne & Pecora, 1976). The analysis of these fluctuations is usually achieved through the normalized time correlation function of the scattered intensity,  $g_2(t)$ , which is related to the time correlation function of the scattered electric field,  $g_1(t)$ , by the Siegert relationship. For monodisperse hard spheres  $g_1(t)$  decays exponentially with time. The decay constant,  $\Gamma$ , allows the determination of the translational diffusion coefficient, according to  $\Gamma = D_{\text{trans}}q^2$ . Therefore, a plot of  $\ln g_1(t)$  vs.  $t$  should give a straight line, although deviations are quite common due to: (i) polydisperse

sample, (ii) rotational diffusion of the particles, and (iii) internal chain dynamics. For polymer molecules an intermediate regime can be found for which the initial decay of the measured intensity autocorrelation function from a cumulant analysis (Koppel, 1972) can be described by

$$D_{\text{ap}}(q) = \frac{\Gamma_1}{q^2} = D_c[1 + k(R_gq)^2 + \dots] \quad (10)$$

where  $\Gamma_1$  is the first cumulant, and  $k$  is a dimensionless quantity which strongly depends on the structure, flexibility and polydispersity of the macromolecule.  $D_c$  is the translational diffusion coefficient of the macromolecule at a finite concentration  $c$ . In most cases, the concentration dependence of the diffusion coefficient can be approximated by a linear relationship

$$D_c = D_{\text{trans}}(1 + k_Dc) \quad (11)$$

Combination of the last equations gives

$$D_{\text{ap}}(q) = D_{\text{trans}}[1 + k_c(R_gq)^2 + \dots](1 + k_Dc) \quad (12)$$

This equation is very similar to that of the SLS equation; when plotted it gives rise to the so called dynamic Zimm plot.

The hydrodynamic effective radius,  $R_h$ , can be calculated applying the Stokes–Einstein relationship

$$D_{\text{trans}} = \frac{K_B T}{6\pi\eta_s R_h} \quad (13)$$

where  $\eta_s$  is the viscosity of the solvent, and  $K_B$  is the Boltzman constant.

## 2. Experimental

### 2.1. Materials

PG (Fluka Biochemika, 95%) was dissolved in water with the addition of NaOH until a pH 7.0 was reached. A stock solution of 4.16 g dm<sup>-3</sup> at pH 6.88 (in 0.0375 g dm<sup>-3</sup> phosphate buffer) containing the antimicrobial NaN<sub>3</sub> (107 ppm) and EDTA (1.04 mmol dm<sup>-3</sup>) was prepared. The last compound was added to prevent gelation by the possible presence of Ca<sup>+2</sup> ions. The stock solution was then stirred for 2 h and passed through 0.45 μm nylon-66 filters (Whatman). Dilutions were made with the buffer solution.

Solutions at pH 3.83 and 3.31 were similarly prepared with the appropriate lactate/lactic solutions. In these cases a small amount of a precipitate appeared which was removed by centrifugation and filtration after stirring for 12 h. The dried precipitate was weighed, permitting determination of the PG concentration in solution.

All solutions were filtered again during the filling of the measurements cells.

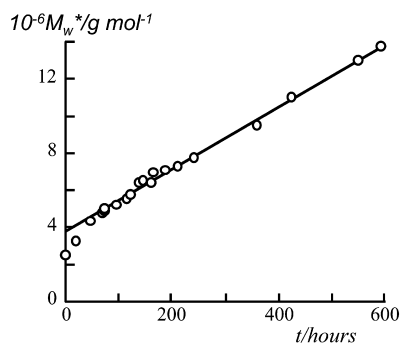


Fig. 2. Dependence of  $M_w^*$  vs. time showing that except at short times the growing rate is constant. [PG] = 2.5 g dm<sup>-3</sup>. pH 3.83.  $T = 25\ ^\circ\text{C}$ .

## 2.2. Light scattering

Light scattering measurements were performed in a Malvern 4700c equipment. The wavelength used was 488 nm and benzene was employed as standard. Scattering data were collected at 25 °C over the angular range 30–140°. Refractive index increment,  $dn/dc = 0.153\ \text{cm}^3\ \text{g}^{-1}$ , was obtained from measurements in a differential refractometer Atago model DD7.

## 3. Results and discussion

### 3.1. Aggregation of PG at pH 3.83

Fig. 1 shows the intensity of scattered light vs.  $q^2$  according to Berry plot (Berry, 1966). The plot shows a good linear behaviour at the lowest  $q$  values from which the radius of gyration and an apparent molecular weight,  $M_w^*(c)$ , can be obtained

$$\frac{1}{M_w^*(c)} = \frac{1}{M_w(c)} + 2A_2c + \dots \quad (14)$$

The measurements were carried out at different times observing a clear increment in the apparent molar mass. The kinetics was followed for 25 days and the results are shown in Fig. 2. It can be observed that  $M_w^*$  increases linearly with time except at the beginning of the experiment. Values of  $1.68 \times 10^4\ \text{g mol}^{-1}\ \text{h}^{-1}$  and  $3.81 \times 10^6\ \text{g mol}^{-1}$  were

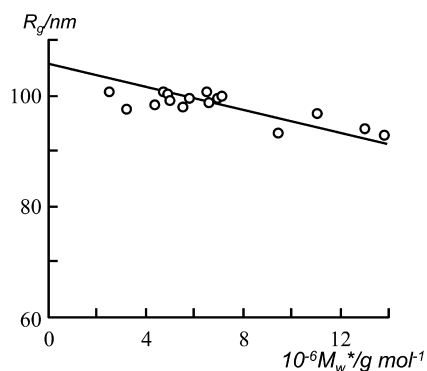


Fig. 3.  $R_g$  vs.  $M_w^*$  for the PG aggregates.

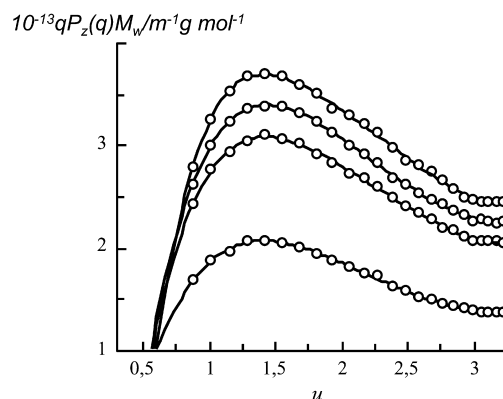


Fig. 4. Casassa–Holtzer plots at different aggregation times (from down to up: 15, 34, 62.7 and 88.8 h). [PG] = 2.5 g dm<sup>-3</sup>. pH 3.83.  $T = 25\ ^\circ\text{C}$ .

obtained for the slope and intercept, respectively. The intercept value does not correspond to  $M_w^*$  at zero time since initially the rate is faster.

It is a surprise that the radius of gyration remained practically constant with time while an extraordinary increase of the molar mass was measured (Fig. 3 plots the dependence of  $R_g$  with  $M_w^*$ ). According to the percolation theory, if the aggregation were a random process, the molecular weight and size of aggregates should grow with a fractal dimension between 2.0 and 2.5 (De Gennes, 1979). Furthermore, the molecular weight and  $R_g$  should be related through a potential law (exponent between 0.4 and 0.5). When an aggregation of stretched chains is considered, once a stick has been constituted, the radius of gyration does not increase although the molecular weight increases. As the radius of gyration describes the distribution of statistics of the particles of mass, a slight decrease of this parameter could lead to increase in mass if the aggregation would be stronger in the central zone than on the ends of the chains. But the increase of  $R_g$  is so slight that during the aggregation process the aggregates remain essentially with the same geometrical shape and contour length. Alternatively, the aggregation could imply the formation of regular star-branched structures. In this case, if the number of arms is larger than  $f = 3$ , the Kratky plot passes through a maximum and approaches a plateau at large  $u$  ( $qR_g$ ). The height of the plateau is  $(6f - 4)/f^2$  (Burchard, 1983) allowing the estimation of the number of arms. Furthermore, the position of the maximum appears very close to  $u_{\text{max}} = 2.45$ . When plotting the experimental results according to Kratky and Porod (1949), an almost linear dependence is observed, and therefore the star aggregation must be ruled out.

If the hypothesis of a lateral aggregation with constant contour length for the aggregates is correct, then the parameter  $\phi$  as well as the number of Kuhn segments, should remain constant during the aggregation process (Schmidt et al., 1985). To test the validity of the hypothesis, the experimental results were plotted according to Casassa–Holtzer (Schmidt et al., 1985). Fig. 4 shows a few examples obtained at different aggregation times. All curves show a

Table 1

Evolution of structural parameters (deduced from Casassa–Holtzer and Berry plots) with time for  $[PG] = 2.5 \text{ g dm}^{-3}$ , pH 3.83,  $T = 25 \text{ }^\circ\text{C}$ .  $M_{w1}$  is  $M_w$  per chain

| Time (h) | $10^{-3} M_{w1}$ (g mol $^{-1}$ ) | $10^{-3} M_L$ (g mol $^{-1}$ nm $^{-1}$ ) | $N_{Kw}$ | $L_w$ (nm) | $l_p$ (nm) | $\phi$ | Aggregation number |
|----------|-----------------------------------|---|----------|------------|------------|--------|--------------------|
| 15.0     | 228                               | 4.4                                       | 4.1      | 572        | 70         | 5.7    | 11.0               |
| 62.7     | 231                               | 7.5                                       | 4.4      | 579        | 66         | 5.9    | 18.9               |
| 83.6     | 242                               | 7.9                                       | 4.5      | 607        | 67         | 6.0    | 19.7               |
| 87.9     | 232                               | 8.5                                       | 4.1      | 584        | 70         | 5.8    | 21.2               |
| 88.8     | 236                               | 8.5                                       | 4.4      | 592        | 67         | 6.0    | 21.3               |
| 150.7    | 237                               | 10.9                                      | 4.3      | 595        | 70         | 5.9    | 27.4               |
| 159.2    | 233                               | 11.3                                      | 4.3      | 585        | 68         | 5.9    | 28.3               |
| 180.4    | 236                               | 11.7                                      | 4.4      | 593        | 68         | 6.0    | 29.5               |
| 200.4    | 231                               | 12.3                                      | 4.4      | 580        | 67         | 6.0    | 30.9               |
| 223.3    | 233                               | 12.6                                      | 4.6      | 586        | 64         | 6.1    | 31.6               |
| 256.1    | 232                               | 13.4                                      | 4.3      | 582        | 67         | 6.0    | 33.6               |
| 373.0    | 216                               | 17.5                                      | 4.2      | 543        | 65         | 5.8    | 43.9               |
| 438.5    | 233                               | 18.9                                      | 4.4      | 585        | 66         | 6.1    | 47.3               |
| 566.8    | 226                               | 22.9                                      | 4.3      | 566        | 66         | 6.0    | 57.6               |
| 607.6    | 216                               | 25.5                                      | 4.2      | 543        | 65         | 5.9    | 64.0               |

maximum at intermediate  $u$  values and reach a plateau at higher  $u$  values. From them, as it was commented on above, the different structural parameters of Table 1 can be deduced.

This table shows that the  $\phi$  parameter values are clearly different from those corresponding to the extreme values for a thin rod (3.5) and a thin prolate ellipsoid (4.5), suggesting a different structure for the aggregates. The parameter, as well as the number of Kuhn segments, is constant with time (or equivalently with the molecular weight of the aggregate). This constancy is in agreement with Eqs. (6) and (7) (corresponding to a wormlike chain and a random coil, respectively) which require a direct relationship between both parameters. By using an average value of  $N_K = 4.3$  deduced from the Table 1, these equations give values for  $\phi$  as 5.1 and 4.6, for the random coil and the wormlike chain, respectively. Both values are too close (and not far from the experimental one,  $\phi_{\text{average}} = 5.9$ ) to distinguish between both structures. However, the existence of the plateau in the Casassa–Holtzer plot suggest the wormlike structure as the most probable one.

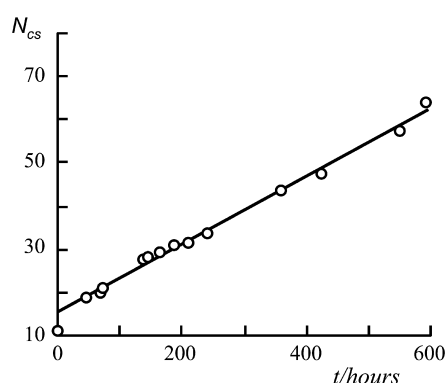


Fig. 5. Evolution of the average number of chains per cross section,  $N_{cs}$ , with time for PG. Experimental conditions as in previous figures.

The average number of chains per cross section in an aggregate,  $N_{cs}$ , can be deduced from the ratio between the mass per unit length of the aggregate and the mass per unit length of a single polygalacturonic chain. The evolution of  $N_{cs}$  with time is shown in Fig. 5. Obviously, the plot is linear indicating again a constant aggregation rate equal to 1.9 chains per day.

After 600 h the experiment was stopped and a classic Zimm plot was measured by diluting the sample from the initial concentration of  $2.5 \text{ g dm}^{-3}$  to a final one of  $0.44 \text{ g dm}^{-3}$ . The obtained results are plotted in Fig. 6. The value deduced for the second virial coefficient is close to zero ( $3.35 \times 10^{-8} \text{ mol ml g}^{-2}$ ) in agreement with the values obtained by Berth, Dautzenberg, & Hartmann (1994) for aggregates of pectins.

The aggregation kinetics can be described in terms of the mean field Smoluchowski equation (Broide & Cohen, 1992; Daoud, 1987; Villarica, Casey, Goodisman, & Chaiken, 1993; Wright, Muralidhar, & Ramkrishna, 1992). Under low concentration conditions where only binary collisions need to be considered and

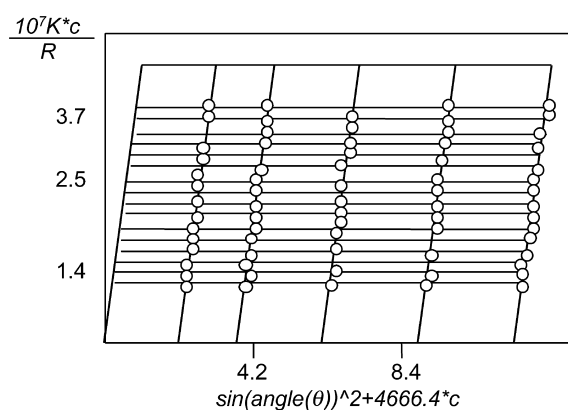


Fig. 6. Zimm plot for PG aggregates formed after 600 h.

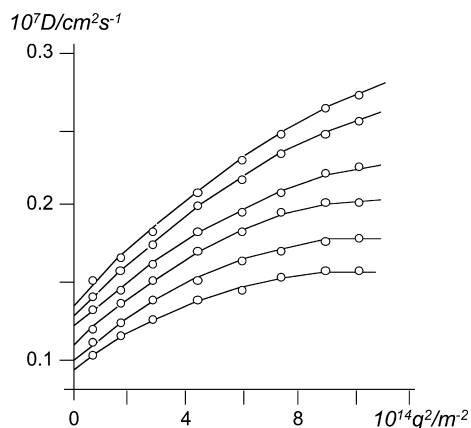


Fig. 7. Time evolution (up to down) of the dependence of the diffusion coefficients with  $q^2$  for PG. Experimental conditions as in previous figures.

assuming that the aggregation is an irreversible process, the kinetic equation has the form

$$\frac{dP_n}{dt} = \frac{1}{2} \sum_{i+j=n} K_{ij} P_i P_j - \sum_{k=1}^{\infty} K_{nk} P_k P_n \quad (15)$$

Here  $P_n$  is the concentration of aggregates (clusters) of size  $n$ , and  $K_{ij}$  are the kinetic constants (in the fractal literature they are known as ‘kernels’) for the association kinetics of aggregates of size  $i$  and  $j$  to form an aggregate of size  $i + j$ . Therefore, the first term in Eq. (15) represents the generation of clusters of size  $n$  from smaller clusters and the second one represents the disappearance of clusters of size  $n$  to form larger clusters of size  $n + k$ . The behaviour of the system is determined by the kinetic constants  $K_{ij}$ . Analytical solutions of Eq. (15) are possible only in certain special cases. The simplest one (considered by Smoluchowski himself) corresponds to the case in which all the kernels are identical and equal to a constant  $K$ . Under this hypothesis the concentration of aggregates of size  $k$  is given by the equation

$$P_k = \frac{T^{k-1}}{(1+T)^{k+1}} \quad (16)$$

where  $T$  is the time in  $K^{-1}$  units. According to this

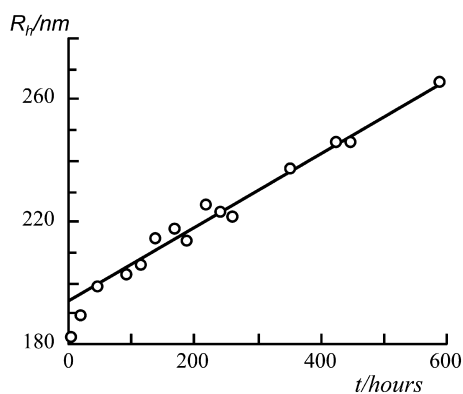


Fig. 8. Hydrodynamic radius vs. time for PG aggregation at pH 3.83.

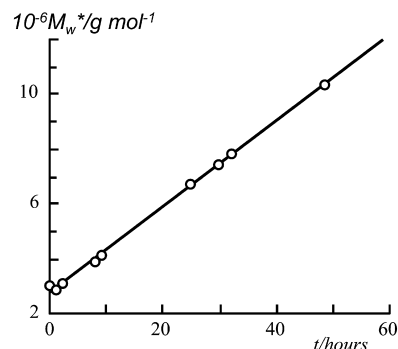


Fig. 9. Dependence of  $M_w^*$  vs. time. [PG] = 2.9 g dm<sup>-3</sup>. pH 3.31.  $T = 25$  °C.

equation the concentration of the aggregates of size  $k$  has a maximum for a time given by  $T = (k - 1)/2$  and the concentration of the monomer decreases steadily. This solution allows to calculate the growth of the number ( $N_n$ ) and the weight ( $N_w$ ) average aggregate mass, the results being

$$N_n = 1 + T \quad (17)$$

$$N_w = 1 + 2T \quad (18)$$

i.e. the growth of the average cluster is linear with time. Therefore the experimental results for the growing of the aggregates (Figs. 2 and 5) can be understood under this simple Smoluchowski model. On the other hand, the polydispersity, defined by the relationship  $N_w/N_n$ , increases with time reaching a maximum value of two at infinite time. This fact is also in agreement with the slight increase of the position of the maximum in the Cassasa–Holtzer plot observed in Fig. 4 (see also Fig. 10 below) in the interval of  $u_{\max} = 1.4$  (for monodisperse chains) and 1.73 (for polydisperse chains), mentioned above.

Fig. 7 resumes the experimental results from QLS experiments. It shows the obtained values for the diffusion coefficients at different times and  $q^2$  values. The lines drawn in the figure correspond to a quadratic fit of  $D$  with  $q^2$ . The hydrodynamic radii were obtained from the  $D$  values at  $q = 0$  and the results are plotted in Fig. 8. This figure shows that the hydrodynamic radius changes linearly with time although the observed change (from 180 to 260 nm) can be considered small.

From the results of Figs. 5 and 8 a linear dependence between the hydrodynamic radius and the average number of chains per cross section can be found, the result being  $R_h = 170 + 1.55N_{cs}$ . The observed slope represents the increase in the hydrodynamic radius when an additional chain incorporates to an aggregate. This value is close to the observed radius for a pectin chain deduced from X-ray experiments carried out by Walkinshaw and Arnott (1981a, b). For an amide pectin (unpublished results) the observed value was 44 nm/chain. These two figures suggest that the aggregation of pectin polymer chains is accomplished by a

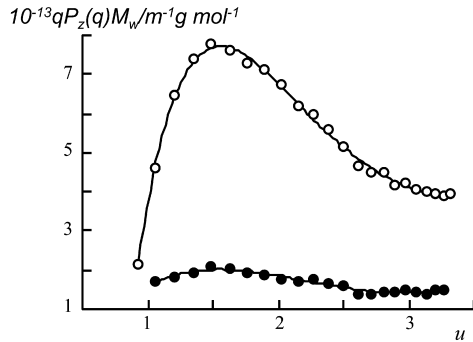


Fig. 10. Casassa–Holtzer plots observed at 25 (●) and 65 (○) min for the aggregation of PG at pH = 3.31. [PG] = 2.9 g dm<sup>-3</sup>.

great number of water molecules which remain trapped into the aggregate (a necessary condition to form hydrogels as it is the actual case for pectins) but not in the aggregation of PG. In fact, PG does not gel at any of the experimental pH values studied here.

### 3.2. Aggregation behaviour of PG at pH 3.31

Similar studies to those described previously were carried out at pH 3.31. Fig. 9 shows the experimental evolution of the apparent molar mass.  $M_w^*$  increases linearly with time much faster than that at pH 3.83, and  $R_g$  remains practically constant, the average value being  $78 \pm 2$  nm. Experiments were stopped after (typically) 60–70 h since a significant fraction of the aggregates precipitated. After this time the solution also acquired a white colour evidencing a sedimentation process.

Only at initial times the Casassa–Holtzer plot evidences the existence of a maximum around  $u_{max} = 1.6$  and a plateau at  $u > 2.7$  (Fig. 10). The values obtained at 25 and 65 min for the average number of chains per cross section in an aggregate,  $N_{cs}$ , were 11.2 and 31.2, respectively. The aggregates grow also in length since values of 533–794 nm were obtained for the contour length. The number of Khun segments also grows and the  $\phi$  parameter changes from 5.62 to 7.71.

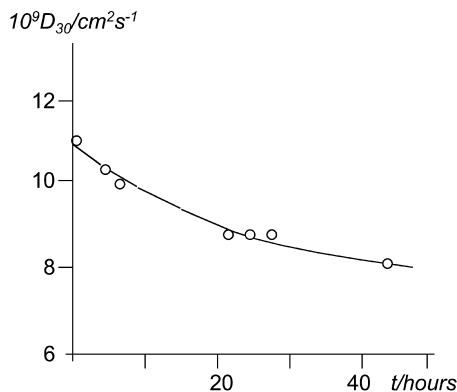


Fig. 11. Time evolution of the diffusion coefficient at 30° for PG aggregation. Experimental conditions as in Fig. 9.

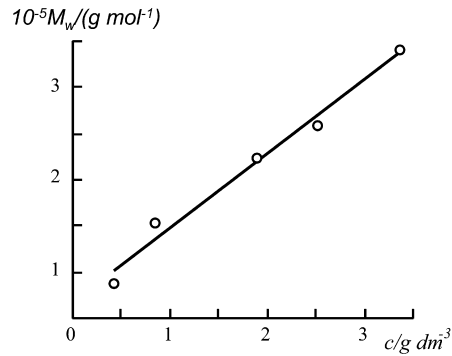


Fig. 12. Dependence of  $M_w$  with PG concentration at pH 6.88.

At longer times the Casassa–Holtzer plots do not evidence (experimental results not shown) the existence of plateaus. However, maxima around  $u_{max} = 1.4–1.8$  were observed. These results suggest a random coil structure for the aggregates. This less ordered structure (compare with the one observed at pH 3.83) would be the result of the faster aggregation observed at this pH value. This fast aggregation of chains would not allow the formation of better ordered structures as wormlike or linear ones, which require a lateral aggregation.

The faster aggregation rate does not allow an accurate determination of the diffusion coefficient at different scattering angles because of the large time necessary for these experiments. For this reason, only values at 30° were obtained, the results being plotted in Fig. 11.

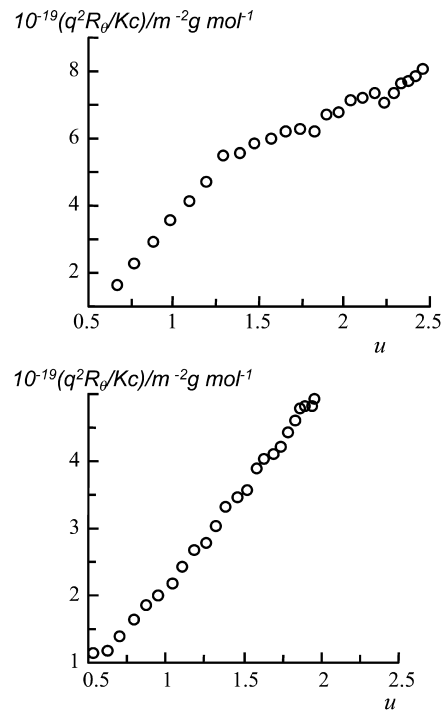


Fig. 13. Kratky plots for PG at pH 6.88 and concentrations of (a) 0.844 and (b) 3.37 g dm<sup>-3</sup>.

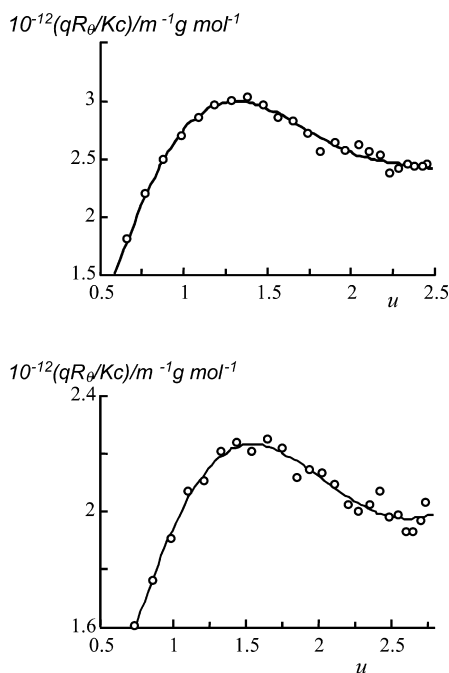


Fig. 14. Casassa–Holtzer plots for PG at pH 6.88 and concentrations of (a)  $3.37 \text{ g dm}^{-3}$  and (b)  $2.53 \text{ g dm}^{-3}$ .

### 3.3. Aggregation behaviour of PG at pH 6.88

At this pH the PG is completely ionized, i.e. is a polyanion. However, the high concentration of salts (to adjust the pH or to prevent mould growth) which give  $[\text{Na}^+] > 0.04 \text{ M}$ , were high enough as to reduce the long range interactions between chains. Therefore its behaviour can be approximated to the one of a neutral polymer chain.

At this pH value no changes with time were observed and only dependences of structural parameters with concentration can be considered. Fig. 12 shows an almost linear dependence of the apparent weight average molecular weight (Eq. (14)) with PG concentration. The extrapolation of the experimental results at zero concentration gives a value of  $M_w = 75 \times 10^3 \text{ g mol}^{-1}$ . The values obtained for the radius of gyration slightly increase with concentration ranging from  $69.9 \text{ nm}$  at  $[\text{PG}] = 0.422 \text{ g dm}^{-3}$  to  $78.5 \text{ nm}$  at  $[\text{PG}] = 3.37 \text{ g dm}^{-3}$ .

As previously, the experimental intensity of light scattered were plotted according to Kratky equation. Two

Table 2

Structural parameters for PG at different polymer concentrations at pH 6.88 and  $25^\circ\text{C}$

| $c \text{ (g dm}^{-3}\text{)}$                    | 0.422  | 0.844 | 1.69 | 2.53 | 3.37 |
|---|--------|-------|------|------|------|
| $M_L \text{ (g mol}^{-1} \text{ nm}^{-1}\text{)}$ | (556)  | 589   | 706  | 785  | 961  |
| $N_{cs}$  | (1.37) | 1.45  | 1.74 | 1.93 | 2.36 |
| $10^{-3} M_{w1} \text{ (g mol}^{-1}\text{)}$      | (64)   | 107   | 129  | 134  | 144  |
| $N_{Kw}$  | (1.5)  | 1.5   | 2.8  | 1.8  | 2.4  |
| $L_w \text{ (nm)}$                                | (158)  | 262   | 316  | 330  | 354  |
| $l_K \text{ (nm)}$                                | (105)  | 175   | 111  | 112  | 148  |
| $l_p \text{ (nm)}$                                | (53)   | 87    | 56   | 56   | 74   |
| $\phi = L_w/R_g$                                  | (3.46) | 3.57  | 4.07 | 4.20 | 4.51 |

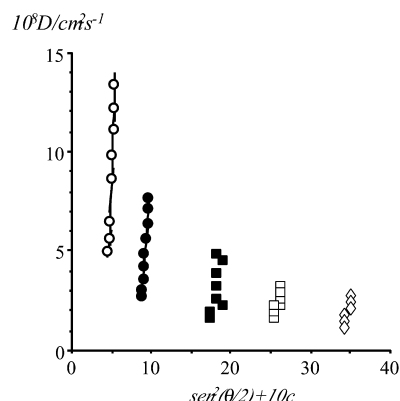


Fig. 15. Quasi-elastic light scattering experiments plotted as a dynamic zimm diagram.

of these plots are shown in Fig. 13 where the absence of a maximum and the asymptotic decrease with  $u$ , suggests that the aggregates structure is not a star-branched one. Again it is concluded that the process implies a lateral aggregation.

This conclusion was confirmed by plotting the results according to Casassa–Holtzer (Fig. 14) which correspond to wormlike structures. From them and following the same calculation process as above, the parameters of Table 2 were derived. For the lowest concentration studied the asymptote was not observed (probably due to the values of  $qR_g$  were not high enough) and values in brackets were derived accepting that the aggregates behave as rigid rods for which the value of  $\phi$  is 3.46. This allows the determination of the contour length and therefore the other parameters as well. The value used for  $\phi$  is also supported by its experimental tendency with concentration. The number of average number of chains per cross section in an aggregate,  $N_{cs}$ , is much lower than that at previous pHs. The low values observed suggest that the polymer chains only interact in the aggregate in less than 50% of their length.

Fig. 15 resumes the quasi-elastic light scattering experiments plotted as a dynamic Zimm diagram. The concentrations studied were the same as those in static measurements. Hydrodynamic radius ( $R_h$ ) were obtained from the Stokes–Einstein equation and diffusion coefficients ( $D$ ) obtained by extrapolation to a zero scattering angle. The results are shown in Table 3 together with the values for Burchard's parameter  $\rho$ . Its dependence with concentration does not allow a direct extrapolation, but the value at zero concentration can be obtained from individual extrapolation of  $R_h$  ( $= 65 \text{ nm}$ ) and  $R_g$  ( $= 22 \text{ nm}$ ). The high resulting value of  $\rho = 2.9$  is only compatible with polydisperse rigid rods (Burchard, 1994a,b) This supports

Table 3

Values for  $D_c$ ,  $R_h$  and  $\rho$  at different PG concentrations at pH 6.88

| $c \text{ (g dm}^{-3}\text{)}$                  | 0.422 | 0.844 | 1.69 | 2.53 | 3.37 |
|---|-------|-------|------|------|------|
| $10^8 D_c \text{ (cm}^2 \text{ s}^{-1}\text{)}$ | 4.86  | 2.49  | 1.63 | 1.42 | 1.12 |
| $R_h \text{ (nm)}$                              | 50    | 98    | 150  | 173  | 218  |
| $\rho$  | 1.39  | 0.75  | 0.52 | 0.45 | 0.36 |

the use of  $\phi$  as 3.46 for the calculations in brackets of Table 2.

### Acknowledgement

We thank the DGICYT (Spain) for financial support (project PB90-0758).

### References

- Berne, B. J., & Pecora, R. (1976). *Dynamic Light Scattering*. New York: Wiley.
- Berry, G. C. (1966). *Journal of Chemical Physics*, *44*, 4550–4564.
- Berth, G., Dautzenberg, H., & Hartmann, J. (1994). *Carbohydrate Polymer*, *25*, 197–202.
- Broide, M. L., & Cohen, R. J. (1992). *Journal of Colloid and Interface Science*, *153*, 493–508.
- Burchard, W. (1983). *Advances in Polymer Science*, *48*, 1–124.
- Burchard, W. (1994a). Light scattering techniques. In S. B. Ross-Murphy (Ed.), *Physical Techniques for the Study of Food Biopolymers*. London: Blackie.
- Burchard, W. (1994b). In S. B. Ross-Murphy (Ed.), *Physical Techniques for the Study of Food Biopolymers*. New York: Chapman and Hall.
- Burchard, W., Schmidt, M., & Stockmayer, W. H. (1980). *Macromolecules*, *13*, 1265–1272.
- Clark, A. H., & Ross-Murphy, S. B. (1987). *Advances in Polymer Science*, *83*, 57–192.
- Daoud, M. (1987). In G. R. Freeman (Ed.), *Kinetics of Non-Homogeneous Processes*. New York: Wiley.
- De Gennes, P. G. (1979). *Scaling Concepts in Polymer Physics*. New York: Cornell University Press.
- Flory, P. J. (1969). *Statistical Mechanics of Chain Molecules*. New York: Wiley.
- Gómez, C., Navarro, A., Manzanares, P., Horta, A., & Carbonell, J. V. (1997). *Carbohydrate Polymers*, *32*, 17–22.
- Holthoff, H., Egelhaaf, S. U., Borkovec, M., Schurtenberger, P., & Sticher, H. (1996). *Langmuir*, *12*, 5541–5549.
- Koppel, D. E. (1972). *Journal of Chemical Physics*, *57*, 4814–4820.
- Kratky, O., & Porod, G. (1949). *Journal of Colloid and Interface Science*, *4*, 35–70.
- Kuhn, W. (1934). *Kolloid-Z.*, *68*, 2.
- Lang, P., & Burchard, W. (1993). *Macromolecules*, *26*, 3992–3998.
- Meakin, P. (1992). *Physica Scripta*, *46*, 295–331.
- Morris, V. J. (1991). In Dickinson, E. (Ed.), *Weak and strong polysaccharide gels*. Food Polymers, Gels and Colloids, Dorchester: Royal Society of Chemistry.
- Rees, D. A. (1969). *Advances in Carbohydrate Chemistry and Biochemistry*, *24*, 267–332.
- Schmidt, M. (1984). *Macromolecules*, *17*, 553–560.
- Schmidt, M., Paradossi, G., & Burchard, W. (1985). *Macromolecular Chemical Rapid Communications*, *6*, 767–772.
- Scurthenberger, P., & Newman, M. E. (1993). Characterization of biological and environmental particles using static and dynamic light scattering. In J. Buffle, & H. P. Van Leeuwen (Eds.), (Vol.2). *Environmental Particles*, Boca Ratón: Lewis.
- Villarica, M., Casey, M. J., Goodisman, J., & Chaiken, J. (1993). *Journal of Chemical Physics*, *98*, 4610–4625.
- Walkinshaw, M. D., & Arnott, S. (1981a). *Journal of Molecular Biology*, *153*, 1055–1073.
- Walkinshaw, M. D., & Arnott, S. (1981b). *Journal of Molecular Biology*, *153*, 1075–1085.
- Wright, H., Muralidhar, R., & Ramkrishna, D. (1992). *Physical Review A*, *46*, 5072–5083.
- Zimm, B. H. (1948). *Journal of Chemical Physics*, *16*, 1099–1116.